

# Vibration Test and Analysis of the NEXIS Ion Engine

John Steven Snyder,\* Anita Sengupta,\* John S. Beatty,<sup>†</sup> Michael R. O'Connell<sup>‡</sup>  
*Jet Propulsion Laboratory, California Institute of Technology, Pasadena, CA, 91109*

Jeff Monheiser<sup>§</sup>  
*Aerojet – General Corporation, Redmond, WA, 98073*

Nils Juhlin<sup>\*\*</sup>  
*NovaComp Engineering, Inc., Bothell, WA, 98041*

and

Brian Sullivan,<sup>††</sup> Michael Collins<sup>‡‡</sup>  
*Materials Research & Design, Inc., Wayne, PA, 19087*

Interest in science objectives at the outer planets, specifically at the moons of Jupiter, has spurred the development of high-power electric propulsion systems under the Prometheus program. As a part of this effort, a JPL-led team has designed, developed, and tested the 20-kW-class NEXIS ion engine. This engine is derived from the proven 30-cm NSTAR engine design and incorporates carbon-carbon ion optics technology to achieve long life. Following the successful performance demonstration of a laboratory model thruster, a Development Model (DM) thruster was designed and fabricated to meet performance and life objectives as well as to survive dynamic and thermal environments. The DM thruster and ion optics were subjected to random vibration testing at protoflight levels in three axes to validate the design and obtain data for dynamic modeling. The NEXIS DM thruster successfully passed the protoflight random vibration testing. Post-test inspection of the thruster showed no damage to any of the components. Ion optics inspection revealed minor adhesive material loss in non-structural bond joints in a few locations. There were no measurable changes in ion optics grid gap or alignment. Measured thruster natural frequencies were similar to, but not in exact agreement with, the predictions of pre-test modeling results using separate dynamically decoupled models. Post-test modeling efforts are underway and preliminary results have demonstrated the necessity of modeling the thruster and ion optics as an integrated unit. Based on the successful results of vibration testing and performance testing, the NEXIS DM thruster design has been demonstrated to be of flight quality.

## I. Introduction

Interest in science objectives at the outer solar system, specifically at the moons of Jupiter, has recently spurred the development of high-power electric propulsion systems. Such missions require high-power, high-Isp thruster operation and long life that represent major increases over the capabilities of state-of-the-art ion engines. For example, preliminary requirements for the proposed Jupiter Icy Moons Orbiter mission are for thrusters that operate at specific impulses of 6000-9000 sec and powers of 20-50 kW with throughputs greater than 2000 kg.<sup>1</sup> As a part of the Nuclear Electric Xenon Ion System (NEXIS) project,<sup>2</sup> a JPL-led team has developed a thruster designed to meet

---

\* Member of the Technical Staff, Advanced Propulsion Technology Group, Member AIAA.

<sup>†</sup> Staff Engineer, Materials Testing and Contamination Control Group, Member AIAA.

<sup>‡</sup> Member of the Technical Staff, Dynamics Environments Group.

<sup>§</sup> Engineering Specialist IV, Systems and Technology Development, Member AIAA.

<sup>\*\*</sup> President.

<sup>††</sup> Director, Member AIAA.

<sup>‡‡</sup> Research Engineer.

the life and performance goals and has demonstrated the required performance in laboratory tests.<sup>3</sup> Two development-model NEXIS thrusters have been fabricated and, as will be demonstrated in this and a companion paper,<sup>4</sup> have met the performance objectives and demonstrated the ability to survive launch loads.

The NEXIS thruster was originally proposed in response to a recent NASA Research Announcement (NRA) which solicited proposals to identify and develop thruster technologies that enable nuclear electric propulsion missions to the outer planets. Under this NRA, the JPL-led team proposed and was awarded funding to develop a thruster with a single-operating-point design at a nominal power of 22 kW, providing a specific impulse of 7500 sec at 78% total efficiency and a throughput of 2000 kg. Later, the NASA Prometheus program was established to develop nuclear power and electric propulsion for exploration. The NEXIS project became part of Prometheus and, along with continued technology development, supported mission planning for the proposed Jupiter Icy Moons Orbiter mission. Performance requirements for NEXIS were transitioned from the original NRA requirements to those for the Prometheus program.

The NEXIS Laboratory Model (LM) thruster was designed to meet the NRA requirements as well as the additional objectives of operation at Isp in the range of 6500 to 8500 sec with high efficiencies at powers of 15 to 25 kW.<sup>3</sup> The LM thruster design is based on the heritage ring-cusp design successfully used in the NSTAR<sup>5</sup> and XIPS<sup>6</sup> ion thrusters, wherein a hollow-cathode discharge is produced in a cylindrical-conical discharge chamber with magnetic multipole confinement of charged particles, and the ion beam is extracted with an electrode set to produce thrust at high Isp. The NEXIS design departs from NSTAR and XIPS with the use of a graphite keeper and carbon-carbon grids to provide the required life. The discharge chamber and magnetic field circuit were designed with physics-based models, validated by test, to provide a high efficiency and flat beam profile. The NEXIS LM thruster design met all of its performance goals for the NRA and the JIMO mission without re-design using experimental iteration. It achieved over 78% efficiency at 7500 sec and 25 kW of power with a beam flatness parameter of 0.82, validating the design tools and methodology and providing useful performance data for mission planners.<sup>3</sup>

Following the success of the LM thruster design and test, the design was transitioned to Development Model (DM) hardware, i.e. hardware that is designed to pass dynamic and thermal environmental testing while meeting all performance and lifetime criteria. Since the LM hardware met all performance objectives, there were no changes to the electromagnetic or fluid designs. In order to meet dynamic requirements, the flat carbon-carbon ion optics were replaced with a dished set of optics specifically designed for vibration tolerance. Performance-based design criteria were handed off to industry, where the mechanical design of the NEXIS DM thruster was completed. Two DM thrusters were fabricated; DM1a has been used for performance and wear testing,<sup>4</sup> and DM1b has been used for vibration testing. The DM1b thruster will later be subjected to post-vibration functional testing.

The focus of this paper is vibration modeling and test of the NEXIS DM1b ion engine. The test had three main objectives: (1) to validate the carbon-carbon ion optics on a valid thruster interface to the Prometheus Electric Propulsion System protoflight random vibration environments; (2) to validate the design and design approaches of the engine and ion optics assembly; and (3) to obtain test data to validate dynamic models of the engine and ion optics. An overview of the NEXIS project, including a discussion of the design and fabrication of the DM, is provided in Ref. 2. Discussion of the carbon-carbon ion optics may be found in Ref. 7. Structural design and analysis of the engine is discussed in Ref. 8. Performance data from the DM1a engine, including initial results from a 2000-hour wear test, are provided in a companion paper.<sup>4</sup>

## **II. Thruster Description and Test Setup**

### **A. Thruster Design and Modeling**

The design philosophy used to generate the NEXIS DM engine was to preserve the critical dimensions determined from the LM thruster design and test (i.e. number and position of the magnet rings, cathode locations, discharge chamber diameter, and active beam area) while building on the successes and lessons learned from other ion thruster developments. In addition, the NEXIS design relied heavily on the heritage of the successful NSTAR ion thruster as well as industry experience in producing flight-qualified electric thrusters. The NEXIS design utilizes machined elements instead of spun-form parts where precise control of the material properties and dimensions are required, and spun-formed parts for those regions where these requirements could be relaxed. The main structural element of the engine is a precision machined ring which could be tightly controlled to ensure structural integrity of the discharge chamber, whereas the rest of the discharge chamber is created from spun-formed conic sections.

Another advantage to the use of a machined element for the main structural member is that small features can be added to the element to significantly increase its stiffness while not significantly increasing the mass of the engine.

Structural analysis of an initial design uncovered an undesirable twisting mode which was prevented by the addition of small flanges to the structural ring in the final design which greatly reduced this motion with negligible mass penalty. Also, to provide strength in the regions where the two of the magnet rings are retained, the material thickness was increased locally. This local control over the part dimensions provides the necessary flexibility to optimize the stiffness of the thruster design without adding a significant amount of unnecessary mass.

As a part of the NEXIS design activities, a full structural analysis of the thruster was conducted to assess its ability to withstand the dynamic and thermal environments. Prior to thruster fabrication, the finite element model shown in Fig. 1 was constructed to represent the thruster design. All structural components from the gimbals to the thruster/optics interface were geometrically represented with elements. The optics assembly was analyzed separately and was included in the thruster model only as a stiff ring with appropriate mass.

The dynamic environment of Ref. 2 was applied in a random vibration analysis for both the thrust and lateral directions. The finite element code NISA was used to compute responses to dynamic inputs using a modal superposition technique on previously extracted eigenvalues. The predicted frequencies of the thruster primary

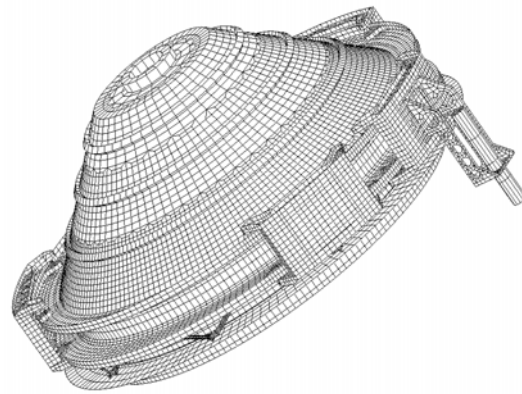


**Figure 1. Finite Element Model of the NEXIS DM Ion Engine.**

**Table 1. Calculated Thruster Natural Frequencies from Thruster Model.**

Mode	Frequency (Hz)	Description
1	90	Chamber cone/cathode
2	97	Neutralizer bracket/chamber cone/cathode
3	107	Neutralizer bracket
4	115	Chamber ring
5	118	Chamber ring
6	120	Neutralizer bracket
7	161	Chamber ring/flexure

modes are listed in Table 1. Positive margins of safety were obtained on all components using the computed three sigma stresses from the random vibration analysis. Results also indicated that displacements were low enough to prevent components in close proximity from contacting one another. The predicted acceleration response of the discharge cathode occurs at frequencies significantly lower than the natural frequencies of its internal components and is therefore considered to be a benign environment for the cathode.

Due to the mismatch in thermal expansion coefficients between the carbon-carbon ion optics and the metallic discharge chamber components, the bipod flexures which form the optics/thruster mechanical interface will experience thermally-induced mechanical loads in the radial direction. The thruster was analyzed for thermal/mechanical responses using a uniform temperature difference between the components. Results indicated that the flexures can accommodate the growth of the metallic thruster without developing significant loads on the optics assembly or in the flexures themselves.

The NEXIS carbon-carbon ion optics assembly is the culmination of several years of development led by JPL, largely building upon the recent successes of the Carbon-Based Ion Optics (CBIO) development of 30-cm ion optics.<sup>9,10</sup> Materials, processes, and lessons learned from that project were incorporated into the NEXIS optics design and fabrication.<sup>7</sup> Production of the NEXIS optics began with a parametric structural analysis using tools developed and validated under CBIO.<sup>2</sup> Those results, coupled with the results of ion optics performance modeling, drove the final grid design. Preliminary dynamic modeling of the optics assembly validated the design.

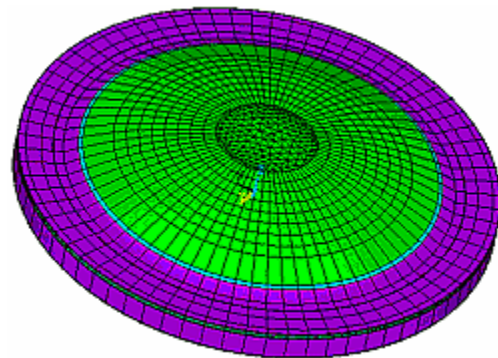


**Figure 2. Finite Element Model of the NEXIS DM Carbon-Carbon Ion Optics.**

Full structural analysis of the ion optics final design using the model shown in Fig. 2 was performed prior to the vibration test using the tools described in Ref. 9 and the vibration spectrum of

Ref 2. The dynamic model is fully 3D with no symmetry assumed, and is built from the optics design drawings. Mode-shape-based damping determined from CBIO testing and also uniform damping levels of 1% were applied in two separate dynamic analyses. In an effort to produce results more representative of the vibration test environment, the optics were subjected to vibration loads calculated from the ion engine structural model at the optics/engine interface instead of applying the random vibration spectrum directly to the optics. The first five natural frequencies calculated for the optics assembly are shown in Table 2. The “safe” grid gap predicted by the analysis, determined by the 99.99% confidence level for no grid-to-grid contact during a full sixty second test, was a factor of three less than the design grid gap. Modest material overstress conditions, compared to calculated material strengths, were predicted in two locations of the screen grid support structure. Because of the conservatism in the model and the assumptions, and the uncertainties in the material damping and vibration input used to produce these results, these overstress calculations were not a source of concern. Materials data acquired after the pre-test modeling and the vibration test was completed confirmed the conservatism. The strength of the carbon-carbon grid material is at least 50% greater than initially assumed.

**Table 2. Calculated Ion Optics Natural Frequencies from Ion Optics Model.**

Mode	Frequency (Hz)
1	401
2	488
3	507
4	515
5	529

**B. Test Article and Equipment**

The NEXIS DM1b thruster served as the test article. The main body of the thruster was the 65-cm-dia. discharge chamber assembly including magnets, gimbal mounts, propellant lines and propellant isolators (note that the propellant supply system in the NEXIS DM models was all-welded). The plasma screen was attached to the chamber structure using riveted nutplates. Mass models were used for both the discharge cathode and neutralizer assemblies. The test article did not include electrical harness. The carbon-carbon ion optics were assembled in the operational configuration and installed on the thruster. A photograph of the instrumented assembly without the plasma screen is shown in Fig. 3. The total mass of the thruster, including ion optics, was 29.1 kg.

Prior to the vibration test, the DM1b engine and ion optics were fully inspected and documented. All engine components were visually inspected during and after assembly, and complete photodocumentation of the engine was performed. Bolts were torqued to specification during assembly. The ion optics were visually inspected and photodocumented before and after assembly. The grid gap and aperture alignment of the assembled optics were inspected. Pre-test optics inspection data are compared to post-test data in Section IIIB.

A total of thirty accelerometers were mounted on the thruster and ion optics for vibration response measurement. The locations of the response accelerometers were chosen based on the pre-test structural model results to facilitate post-test analyses. Five tri-axial accelerometers were mounted on the thruster: two on the main structural member of the discharge chamber, and one each on the neutralizer mounting bracket, the cathode adaptor flange, and one of the two high-voltage propellant isolators. Tri-axial accelerometers were also located on the vibration fixture and on one force transducer adaptor plate which was located between the thruster and vibration fixture. Three uni-axial accelerometers were mounted inside the thruster discharge chamber cylindrical segment, oriented radially and aligned with the three gimbal mount pads. All thruster accelerometers were bonded directly to thruster surfaces with epoxy and additionally restrained by metallic tape.

Twelve PCB 352M123 uni-axial accelerometers were bonded directly to the carbon-carbon ion optics surfaces with epoxy, oriented normal to the optics surfaces. On the screen grid assembly, four were placed on the thruster mounting ring and one on the upstream surface of the screen grid itself on the non-perforated, non-dished region. Six accelerometers were bonded to the dished, perforated area of the accelerator grid, and one on the flat non-perforated section of the grid near the structure periphery. An electrical circuit designed to indicate grid-to-grid contact during vibration testing<sup>9</sup> was also planned for the test. Unfortunately, the instrumentation and test facility

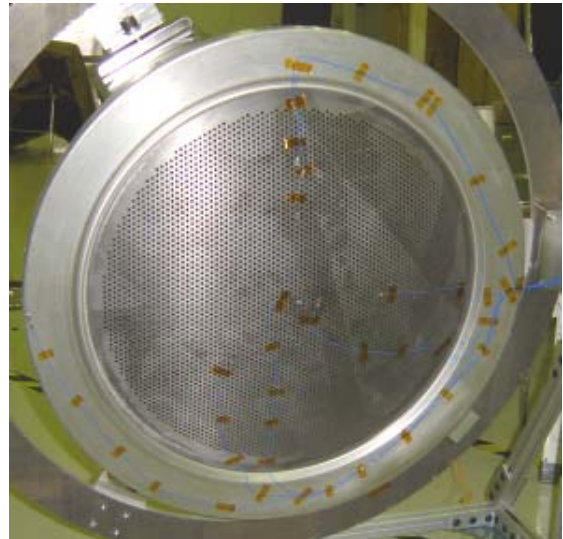


**Figure 3. NEXIS Development Model Thruster DM1b Instrumented for Vibration Test.**

data system were not compatible with the electrical isolation of the grids necessary for the grid contact circuit, so the circuit was ultimately not used.

In lieu of a thruster gimbal assembly, a vibration fixture was designed to provide a rigid interface between the thruster and the facility vibration table. The 122-cm-dia. fixture was fabricated from a single piece of aluminum block. Design and analysis tools were used to ensure sufficiently high stiffness over the test frequency spectrum such that the fixture did not introduce additional modes into the system. In order to minimize fixture mass, the engine was mounted in a downward orientation, i.e. the ion optics were at the bottom of the assembly immediately above the vibration table. The thruster was mounted to the vibration fixture at its three gimbal mount locations. A positive stopping feature was included in the thruster mount design to prevent accidental contact with the table during assembly. A Kistler model 9067 piezoelectric three-axis force transducer was also fastened directly between the thruster and vibration test fixture at each of the three mounting points.

Vibration testing was performed in the JPL Dynamics Environmental Test Facility. The facility includes a Ling Electronics model A249 as the vibration exciter with power amplification provided by a LDS model DPA 180 solid state. Vertical (i.e. Z-axis, or thrust axis) excitation was performed on a Kimball head expander and lateral (X- and Y-axis) excitation on a large oil-lubricated slide plate. Data acquisition from control and response accelerometers was provided at a 20 kHz sampling rate. A photograph of the engine in its final configuration for X-axis excitation is shown in Fig. 4.

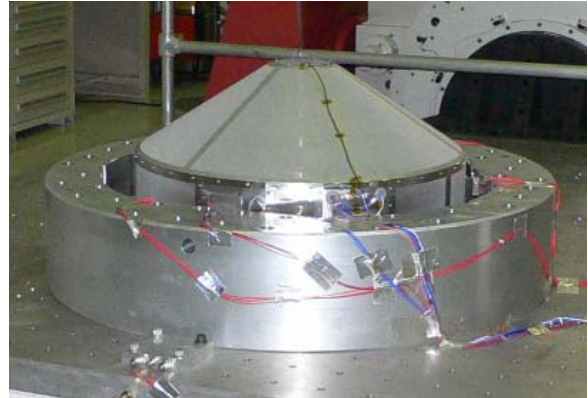


**Figure 4. Test Configuration For X-Axis Excitation.**

### III. Vibration Testing

The random vibration specification for the NEXIS thruster test was developed under the Prometheus program, based on Delta-class launch vehicles and typical locations of electric propulsion hardware on spacecraft. The spectrum used for the testing described herein is slightly different than the spectrum used in the early stages of thruster development.<sup>2,8</sup> It was developed for application to thruster/gimbal assemblies, but was applied to the NEXIS engine through the vibration fixture alone because gimbal development was not a part of the NEXIS project. The protoflight specification, shown in Table 3, has a total level of 10.0 Grms and calls for random vibration testing in each of three orthogonal axes for a duration of sixty seconds per axis.

**Table 3. Protoflight Random Vibration Spectrum.**

Frequency (Hz)	Specification
20	0.04 G <sup>2</sup> /Hz
20 – 50	+ 3 dB/Octave
50 – 600	0.1 G <sup>2</sup> /Hz
600 – 2000	- 6 dB/Octave
2000	0.009 G <sup>2</sup> /Hz
Overall	10.0 Grms

Vibration testing of the NEXIS engine also incorporated the practice of force-limited vibration testing which is used for most vibration tests performed at JPL. Force-limiting during vibration testing guards against artificial test failures caused by overtesting, a result of the infinite mechanical impedance of the shaker and the use of only acceleration-based control. In this situation, the reaction forces at the fixture/engine interface can become unrealistically high compared to a flight environment at test article resonances. In a force-limited test, real-time force measurement and limiting is performed to notch the input acceleration spectrum. Force-limited vibration testing is discussed in more detail in Ref. 11.

Vibration testing in the Z-axis (i.e. thrust axis) was performed first. The first activity was a sine survey of the thruster over the frequency range of 5 to 1500 Hz at a load of 0.25 G<sub>0,pk</sub> and a sweep rate of two octaves per minute (all surveys were truncated at 1500 Hz instead of the standard 2000 Hz to eliminate control difficulties with a vibration fixture mode at 1700 Hz). This was followed by a random vibration test at a level of -18 dB with respect to the full random vibration load. This short, low-level test was performed in order to verify instrumentation operation and tune the vibration force-limiting algorithms. The random vibration test at the full load was then conducted for sixty seconds, followed by a post-random sine survey. After the Z-axis testing was completed the

vibration test facility was reconfigured for lateral excitation and the above process was repeated for the X- and Y-axes.

### A. Test Results

Random vibration testing at the specified protoflight vibration spectrum was successfully performed and completed for all three axes. Testing in each of the lateral axes was completed in single sixty-second test runs; the Z-axis test achieved a total test duration of sixty seconds during three separate test runs due to two instrumentation test aborts. The vibration test inputs, which were notched automatically and in real-time during the test according to the force limit specifications, are compared to the force limit specifications, are compared to the protoflight vibration spectrum in Fig. 5 (there was little difference between the force-limited X and Y axis inputs). Significant notches occurred at 120 Hz for the Z-axis test and 200 and 300 Hz for the lateral axis tests, preventing non-realistic overtesting of the thruster.

Comparison of in-axis sine-survey data acquired before and after the Z-axis and Y-axis random vibration tests showed no significant changes in frequency or gain for all accelerometers. An example is shown in Fig. 6 for the in-axis force for the Z-axis test. Sine survey comparisons from the X-axis test, however, showed minor shape changes at 200 Hz, the first high-mass participation, with a frequency shift down to 194 Hz (i.e. a 3% change) as seen in Fig. 7. There were also some signature changes at frequencies above 1000 Hz. The changes at 200 Hz were observed throughout all accelerometers on the thruster, were associated with the first mode with high mass participation, and were therefore likely associated with the mounting plates at the force transducers located in between the thruster and vibration fixture. Post-test visual inspection of accessible areas of the thruster and ion optics indicated no damage to the hardware. After evaluation of the data and inspection of test hardware, it was concluded that these changes were not structurally significant. It should be noted that this evaluation method and conclusion, based on the available evidence, is not uncommon for vibration tests on JPL flight hardware.

Response data for selected accelerometers on the thruster body are shown in Table 4 for each of the three excitation axes. The in-axis propellant isolator and the Z-axis front mask accelerometer responses typically had the highest levels in each test, likely because of the

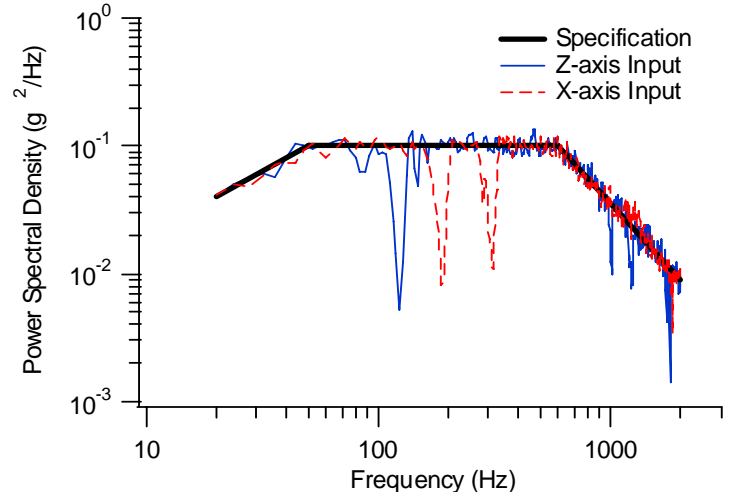


**Fig. 5. Comparison of Force-Limited Test Inputs with Random Vibration Specification.**

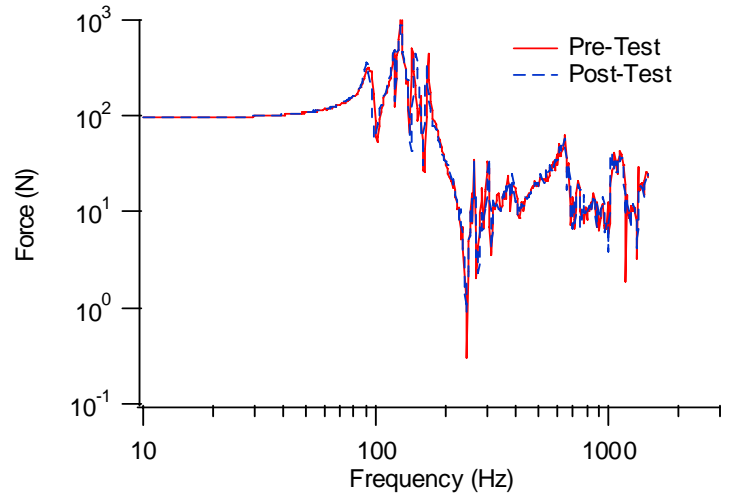


**Fig. 6. Comparison of Sine Survey Results for Z-Axis In-Axis Force.**

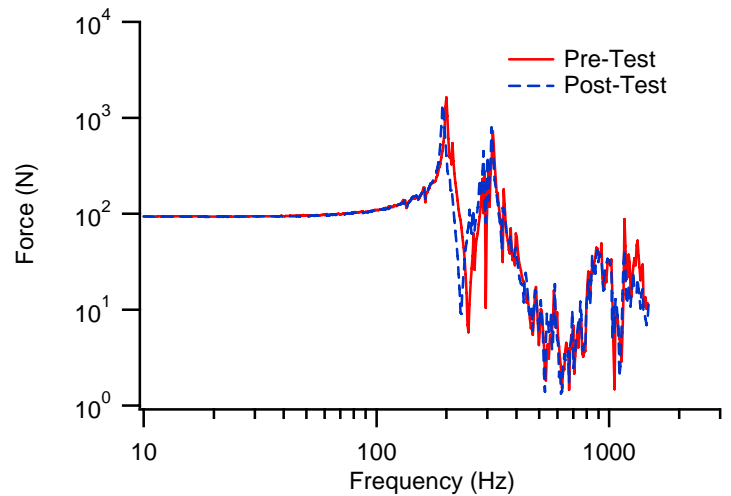


**Fig. 7. Comparison of Sine Survey Results for X-Axis In-Axis Force.**

**Table 4. Random Vibration Response Levels for Thruster Body.**

Accelerometer Mounting Location	Accelerometer Orientation	Response to Z-Axis Stimulation (Grms)	Response to X-Axis Stimulation (Grms)	Response to Y-Axis Stimulation (Grms)
Discharge Chamber Interior, Aligned with Gimbal Pad #1	Along Thruster Radius	26.8	24.5	24.0
Discharge Cathode Flange	Along Excitation Axis	40.5	13.1	14.6
Neutralizer Mounting Bracket	Along Excitation Axis	11.5	14.6	13.1
High-Voltage Propellant Isolator	Along Excitation Axis	58.2	38.0	14.0

cantilevered support configurations of those parts. Response levels on other parts of the thruster body were more modest. In-axis power spectral density data for Z-axis excitation are shown in Fig. 8 for the cathode flange and the main structural member of the discharge chamber. The first mode of the thruster, a chamber cone/cathode mode at 90 Hz, is clearly seen in the cathode flange data.

Response data for selected accelerometers on the ion optics are shown in Table 5 for each of the three excitation axes. Recall that all accelerometers on the ion optics were uniaxial and oriented normal to grid surfaces, i.e. exactly or roughly in the Z-axis. The highest response for all three axes was on the flat periphery of the accelerator grid, at the same radial distance as the fasteners in the insulator assemblies. The highest response on the screen grid was in the flat periphery of the grid just inside the inner diameter of the mounting structure. Excitation in the Y-axis produced essentially the same responses as X-axis excitation for all accelerometers, with some modest differences such as for the screen grid flat periphery as shown in the table.

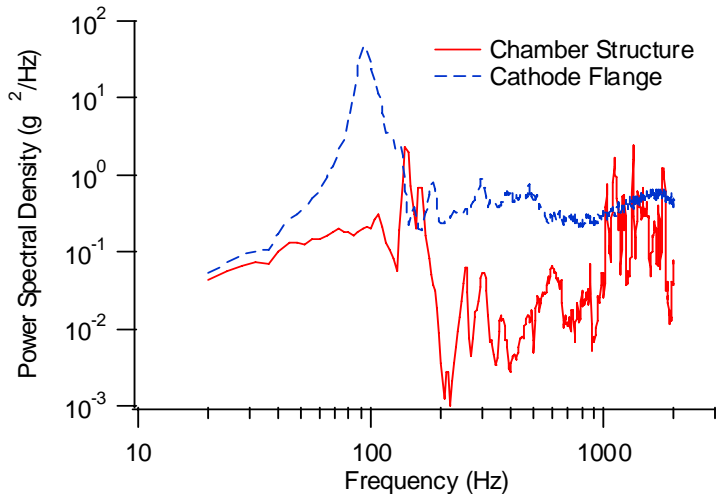


**Fig. 8. In-Axis Response of Thruster Body Accelerometers to Z-Axis Excitation.**

A comparison of the power spectral density data acquired on the accelerator grid centerline is shown in Fig. 9 for Z-axis and X-axis excitation. The similarities of the responses to excitation in the two different directions is interesting. The X-axis RMS response was 23% lower than for the Z-axis, and it is clear that the difference occurred mostly at frequencies less than 250 Hz. The response over the range of ion optics natural frequencies is nearly identical. This indicates that analysis of ion optics in the thrust axis alone does not necessarily represent the worst case for structures of the NEXIS design. In fact, all five of the accelerometers on the screen grid assembly measured higher RMS responses during lateral excitation than in Z-axis excitation. Excitation in the Y-axis produced essentially the same responses as X-axis excitation, with some modest differences. In the absence of a grid-to-grid contact circuit, time-domain data from the accelerometer on the accelerator grid centerline were examined for the Z-

**Table 5. Random Vibration Response Levels for Ion Optics.**

Accelerometer Mounting Location	Response to Z-Axis Stimulation (Grms)	Response to X-Axis Stimulation (Grms)	Response to Y-Axis Stimulation (Grms)
Accelerator Grid Centerline	32.8	25.3	24.9
Accelerator Grid Flat Periphery	43.5	54.6	53.9
Screen Grid Flat Periphery	31.4	34.7	42.5
Screen Grid Mounting Structure	22.9	25.8	25.7

axis random vibration test. Inspection of the time history data revealed no indication that grid-to-grid striking had occurred during the test. While severe clashing would certainly have been detected, the threshold for detection using this method is unknown.

### B. Post-Test Inspection

After testing was completed the thruster was disassembled and inspected. There was no visible damage to any portion of the thruster; inspection of the insulators revealed no chips or cracks. Visual inspection of the ion optics assembly indicated some minor, localized loss of excess bond joint adhesive in five locations near optics mounting bolts. This is not expected to have an effect on the structural integrity of the optics. Other than this, there was no visible damage to any portion of the ion optics assembly. The ion optics dimensional inspection was repeated and compared to the values measured before the vibration test. Normalized grid gap, i.e. the measured gap divided by the design gap, is compared in Table 6 for the pre-test and post-test measurements at the grid centerline and periphery of the perforated region. The results indicate no measurable change in grid gap. Aperture alignment data were measured for several apertures across a grid radius with a

**Table 6. Comparison of Pre- and Post-Test Normalized Grid Gap.**

Location	Pre-Test	Post-Test
Centerline	1.00 ± 0.04	1.04 ± 0.04
Periphery	0.96 ± 0.04	0.96 ± 0.04

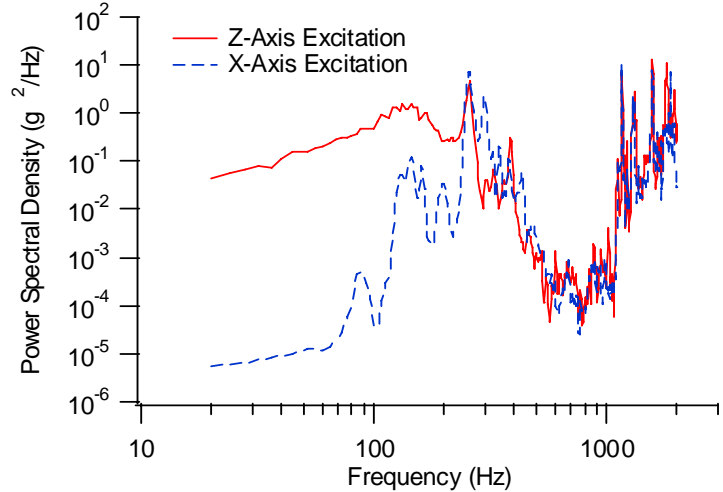


**Fig. 9. Response at Accelerator Grid Centerline to X- and Z-Axis Excitation.**

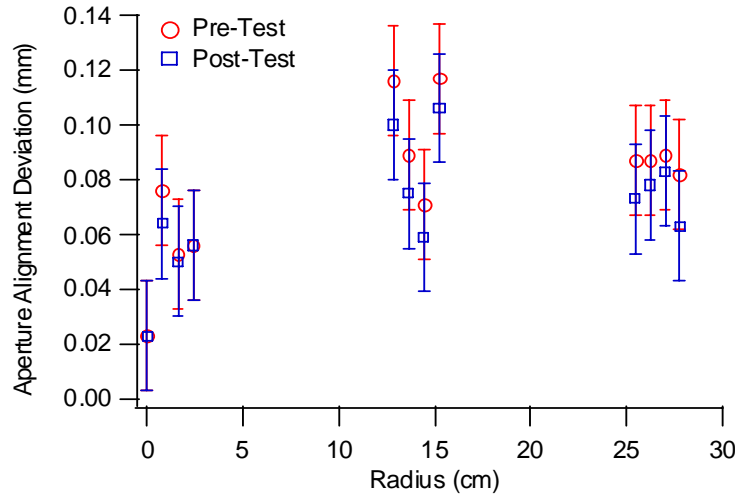


**Fig. 10. Comparison of Pre-Test and Post-Test Aperture Alignment Measurements.**

CMM contact measurement and were calculated as distance between hole centers in a plane tangent to the accelerator grid. The data, compared in Fig. 10 for the pre- and post-test measurements, indicate no change in alignment within the 20- $\mu$ m error in the measurement.

## IV. Post-Test Modeling and Analysis

Initial attempts to perform post-test analysis using the separate thruster and ion optics finite element models were unsuccessful in matching the measured natural frequencies of those structures. This was most likely due to sufficiently strong coupling of the dynamic response between them. Hence, a combined thruster/optics model was created by merging the models independently developed by two different modeling teams. The capabilities of the ion optics portion of the model have also been improved with recently-acquired materials properties data obtained from carbon-carbon witness panels processed along with the NEXIS ion optics. Initial results from the combined finite element model, depicted in Fig. 11, have been obtained and agree well with measured values. A comparison of the first few measured and calculated modes for each structure, obtained from the combined model, is shown in Table 7. Note that the first mode of the engine is not significantly different than predicted by the thruster-only model (shown in Table 1). The combined model correctly predicts a natural frequency at 143 Hz that is observed in the chamber structure data shown in Fig. 8 but not predicted in the thruster-only model. The first natural frequency

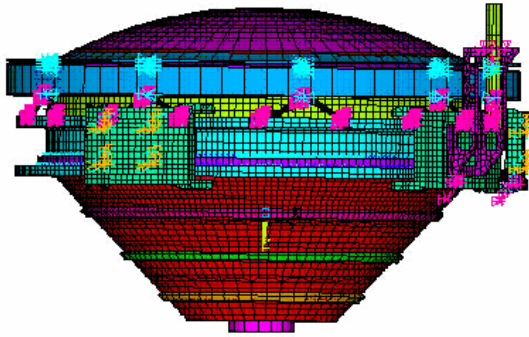


**Fig. 11. Combined Thruster and Ion Optics Finite Element Model.**

**Table 7. Comparison of Measured and Calculated Natural Frequencies Using Combined Thruster/Optics Model.**

	Measured (Hz)	Calculated (Hz)
	92.0	93.4
Thruster Modes		102.2
		102.9
	127.7	121.4
		137.6
	142.5	142.6
Ion Optics Modes	465.6	462.3
	494.3	482.3
	514.4	514.9
		515.5
		519.3
		524.7

of the ion optics predicted with the combined model is about 15% greater than that calculated with the optics-only model. This is at least in part due to the use of the materials properties measured for the grid material, including a greater stiffness than was originally assumed. The next few natural frequencies of the ion optics are very similar to those calculated with the optics-only model.

With the development of the combined and fully coupled model of the thruster and ion optics the post-test analysis will continue with mode correlation to ensure that the primary modes observed during test can be predicted by an eigenvalue analysis of the model. Both the sine survey and random vibration environments will be used for model correlation (e.g. data of Figs. 6-9 and Tables 4 and 5). The random vibration excitation used for post-test modeling will be the measured force-limited control acceleration data shown in Fig. 5. A modal superposition method will be used to calculate the dynamic responses at the accelerometer locations. This method only permits the use of modal damping, so damping can only be modified on a mode by mode basis in order for predicted response power spectral density levels to agree with test data. Achieving agreement between test data and the combined finite element model will help develop critical modeling techniques that can be used on future thruster and ion optics designs. The results of these efforts will be presented in a forthcoming paper.

## V. Conclusion

The NEXIS Development Model ion engine successfully passed vibration testing at Prometheus project protoflight specifications for the electric propulsion subsystem. The engine, including carbon-carbon ion optics, was subjected to random vibration at 10-Grms for sixty seconds in each of three orthogonal axes. Comparison of pre- and post-test sine survey data for each test axis indicated no damage to the thruster assembly. Post-test disassembly and inspection of the thruster revealed no damage. There were no measurable changes in grid gap or aperture alignment for the ion optics. Post-test visual inspection of the ion optics assembly indicated some minor, localized loss of bond joint adhesive in five locations near optics mounting bolts. Initial post-test analysis indicated that separate modeling of the thruster and ion optics did not sufficiently describe the dynamic response of the assembly. A combined thruster/optics finite element model was generated and preliminary calculations are in good agreement with the test data. Based on the successful vibration testing and performance testing, the NEXIS DM ion engine has been demonstrated to be of flight quality.

## Acknowledgments

The research described in this paper was carried out by the Jet Propulsion Laboratory, California Institute of Technology, under a contract with the National Aeronautics and Space Administration in support of Project Prometheus.

## References

1. Oleson, S.R., "Electric Propulsion Technology Development for the Jupiter Icy Moons Orbiter Project," AIAA 2004-5908, Space 2004 Conference and Exhibit, San Diego, CA, Sept. 2004.
2. Randolph, T.M. and J.E.Polk, "An Overview of the Nuclear Electric Xenon Ion System (NEXIS) Activity," AIAA 2004-5909, Space 2004 Conference and Exhibit, San Diego, CA, Sept. 2004.
3. Goebel, D.M., J.E. Polk, and A. Sengupta, "Discharge Chamber Performance of the NEXIS Ion Thruster," AIAA 2004-3813, 40<sup>th</sup> Joint Propulsion Conference, Fort Lauderdale, FL, July 2004.
4. Polk, J.E., D.M. Goebel, J.S. Snyder, A.C. Schneider, and A. Sengupta, , "NEXIS Ion Engine Performance and Wear Test Results," AIAA-2005-4393, to be presented at the 41<sup>st</sup> Joint Propulsion Conference, Tucson, AZ, July 2005.
5. Brophy, J.R., "NASA's Deep Space 1 Ion Engine," Review of Scientific Instruments, Vol. 73, No. 2, Feb. 2002, pps. 1071-1078.
6. Beattie, J.R., "XIPS Keeps Satellites on Track", The Industrial Physicist, June 1998.
7. Beatty, J.S., J.S. Snyder, and W. Shih, "Manufacturing of 57cm Carbon-Carbon Composite Ion Optics for the NEXIS Ion Engine," AIAA 2005-4411, to be presented at the 41<sup>st</sup> Joint Propulsion Conference, Tucson, AZ, July 2005.
8. Monheiser, J., J.E. Polk, and T.M. Randolph, "Conceptual Design of the Nuclear Electric Xenon Ion System," AIAA 2004-3624, 40<sup>th</sup> Joint Propulsion Conference, Fort Lauderdale, FL, July 2004.
9. Snyder, J.S. and J.R.Brophy, "Performance Characterization and Vibration Testing of 30-cm Carbon-Carbon Ion Optics," AIAA 2004-3959, 40<sup>th</sup> Joint Propulsion Conference, Fort Lauderdale, FL, July 2004.
10. Snyder, J.S., J.R. Brophy, D.M. Goebel, and J.S. Beatty, "Development and Testing of Carbon-Based Ion Optics for 30-cm Ion Thrusters," AIAA 2003-4716, 39<sup>th</sup> Joint Propulsion Conference, Huntsville, AL, July 2003.
11. NASA-HDBK-7004B, "Force Limited Vibration Testing," NASA Technical Handbook, January 31, 2003.